Pressure Dependence of Steam / Supercritical Water Oxidation of 9Cr and 18Cr Steels

Yoshiaki Toda [1,*], Nina Kobata [1], Xianglan Li [1] and Masahiko Demura [1]

[1] National Institute for Materials Science, 1-2-1, Sengen, Tsukuba, Ibaraki 305-0047, JAPAN

e-mail: TODA.Yoshiaki@nims.go.jp

1. INTRODUCTION

Understanding the steam oxidation behavior of heat-resistant materials is important for the safe long-term operation of boilers and pressure vessels. Therefore, many studies have been conducted on the oxidation behavior of heat-resistant steels in high-temperature steam. In recent years, in high-efficiency thermal power plants, supercritical water above 600 °C and above 25 MPa is generated in boilers to drive power generation turbines. Furthermore, in light water reactors and geothermal power generation, which are effective for achieving carbon neutrality, the use of supercritical water is also expected. Therefore, it is important to understand not only the oxidation of heat-resistant steels in high-temperature steam but also that in supercritical water. In this study, to investigate the effect of pressure on the oxidation behavior of heat-resistant steels, 9Cr ferritic/martensitic steel and 18Cr austenitic steel were exposed at 650 °C to steam (0.5 MPa), subcritical water (10.2 MPa), and supercritical water (22.7 MPa) for various durations. The time-dependent change in oxide scale thickness associated with oxidation was measured, and the pressure dependence of the oxidation rate constant for each specimen was evaluated.

2. EXPERIMENTAL

9Cr-1Mo-V-Nb ferritic/martensitic steel (9Cr steel) and 18Cr-8Ni austenitic stainless steel (18Cr steel) were investigated. Strip-shaped specimens with dimensions of 20×10×2 mm were cut from these commercial plates. All surfaces of the specimens were mechanically polished and then cleaned and degreased using an ultrasonic cleaner. The specimens were placed in a vertical cylindrical pressure vessel made of nickel-based alloy with a volume of 2.8 L. While heating the pressure vessel in an electric furnace, pure water with a dissolved oxygen content of 15 ppb or less and an electrical conductivity of 10 mS/m or less was supplied to the pressure vessel using a high-pressure pump. When the pressure vessel was heated to 650 °C, the pressure inside the vessel reached 0.5 MPa. By keeping the high-pressure pump operating and closing the back-pressure valve, the pressure vessel was further pressurized and filled with subcritical water (10.2 MPa) or supercritical water (22.7 MPa). The specimens were exposed to these environments for 0 h (in this case, only heating/pressurizing and cooling/depressurizing were conducted), 20 h, 50 h, 72 h, and 195 h. After oxidation for a certain period, the pressure vessel was cooled to 200 °C and depressurized to atmospheric pressure. Subsequently, the steam in the pressure vessel was replaced with argon gas, and the vessel was cooled to room temperature. The specimens were then removed from the pressure vessel, embedded in a resin, and sectioned using a low-load precision cutting machine. The cross-sections of the oxide scales formed on the specimen surfaces were observed using secondary electron images obtained by scanning electron microscopy (SEM, Hitachi Ltd. S-4700).

3. RESULTS AND DISCUSSION

Figure 1 shows the change in oxide scale thickness with oxidation time for (a) 9Cr steel and (b) 18Cr steel in steam (0.5 MPa), subcritical water (10.2 MPa), and supercritical water (22.7 MPa), indicated by triangles, circles, and squares, with a close symbol and an open symbol, respectively. The open symbols are suspected to be underestimated based on the surrounding trends and are therefore excluded from the regression analysis described later. During the heating/pressurizing and cooling/depressurizing processes before and after the oxidation tests, the specimens are also oxidized and oxide scales are formed. Therefore, even at an oxidation time

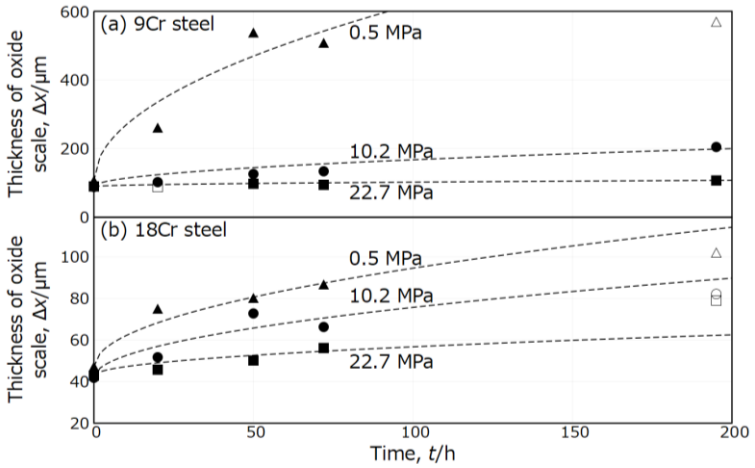


Fig. 1. Change in oxide scale thickness with oxidation time for (a) 9Cr steel and (b) 18Cr steel in steam (0.5 MPa), subcritical water (10.2 MPa), and supercritical water (22.7 MPa) at 650 °C, together with their regression curves.

of 0 h, the oxide scale thickness is not 0 μm. The oxide scale thickness of 9Cr steel is larger than that of 18Cr steel at all pressures. For both steels, the thickness is the largest in steam, followed by subcritical water and supercritical water in decreasing order.

The change in oxide scale thickness x with time t is often described by the following equation.

$$\left(x - x_0\right)^n = k_x t \qquad (1)$$

where x_0 is the oxide scale thickness at an oxidation time of 0 h, n is the reaction exponent, and k_x is the oxidation rate constant determined from the oxide scale thickness. The value of n was obtained from the slope of the regression line by performing linear regression on the log–log plot of oxide scale thickness $x - x_0$ versus time t shown in Fig. 1. Under the steel grades and pressure conditions investigated in this study, n was approximately 2. Therefore, the k_x was calculated from the experimental data of $x - x_0$ and t assuming $n = 2$. The dotted curves in Fig. 1 represent the parabolic curves of Eq. (1) drawn using the obtained k_x with the assumption of $n = 2$. It is found that the time dependence of the oxide scale thickness can be described by Eq. (1).

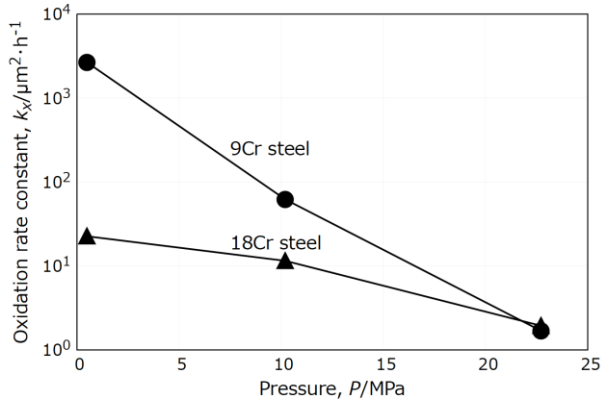


Fig. 2. Pressure dependence of the oxidation rate constant determined from the oxide scale thickness of 9Cr steel and 18Cr steel at 650 °C.

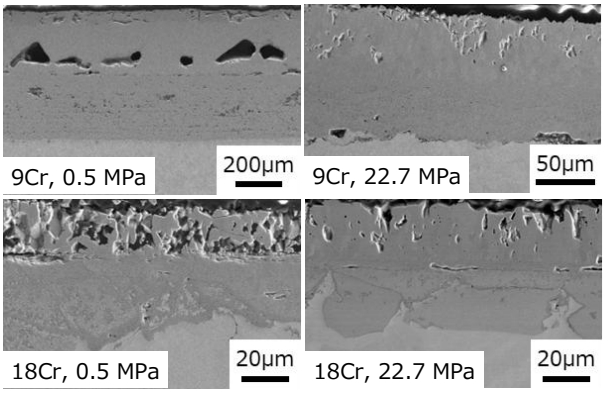


Fig. 3. Cross-sectional SEM micrographs of the oxide scales for 9Cr steel and 18Cr steel after exposure for 50 h in steam (0.5 MPa) and supercritical water (22.7 MPa).

Figure 2 shows the pressure dependence of the oxidation rate constant of 9Cr steel and 18Cr steel, indicated by a close circle and a close triangle, respectively. With increasing pressure, the oxidation rate constants of both steels decreased monotonically. The degree of decrease is larger for 9Cr steel than for 18Cr steel. Notably, in supercritical water, the oxidation rate constants of 9Cr steel and 18Cr steel converged to nearly the same value. Thus, oxidation is significantly suppressed in supercritical water, and the difference between the two alloys disappears.

Figure 3 shows cross-sectional SEM images of the oxide scales of 9Cr steel and 18Cr steel after exposure for 50 h in steam (0.5 MPa) and supercritical water (22.7 MPa). The composition and structure of the oxide scales were analyzed using an energy-dispersive X-ray spectroscopy attached to the SEM and a Raman spectrometer. For 9Cr steel, magnetite-type Fe_3O_4 formed in the outer layer and magnetite-type $(Fe, Cr)_3O_4$ with dissolved chromium formed in the inner layer at both pressures. For 18Cr steel, magnetite-type Fe_3O_4 formed in the outer layer and spinel-type $FeCr_2O_4$ formed in the inner layer at both pressures. In the oxide scale of 9Cr steel formed in steam, large voids exceeding 100 μm were observed in the outer layer rather than near the center. In contrast, the oxide scale formed in supercritical water contained only clearly smaller voids. Similarly, in 18Cr steel, many voids were observed in the outer layer of the oxide scale in steam, whereas the oxide scale in supercritical water contained fewer voids.

4. CONCLUSION

It is suggested that if boilers and pressure vessels are designed based on the oxidation behavior of heat-resistant steels in atmospheric-pressure steam, they can be safely operated using subcritical water or supercritical water at higher pressures at the same temperature. The decrease in the oxidation rate constant with increasing pressure is considered to be due to the reduction in voids in the formed oxide scale, which decreases the contact area between the metal and dissolved oxygen in steam or supercritical water.

Acknowledgements

This study was carried out with the support of JSPS KAKENHI Grant Number 25K08550 and the 35th ISIJ Research Promotion Grant.